High-resolution camera for SAM: instrument manual

Author:*A. Tokovinin*
Revised by:
Version: 2.1
Date: May 29, 2008
File: hrcam/doc/hrcaminst.tex

1 What is HRCam?

High-resolution camera (HRCam) is a fast imager designed to work at the SOAR telescope, either with the SOAR Adaptive Module (SAM) or as a stand-alone instrument. HRCam uses the CCD detector with internal electrom multiplication – a EMCCD.

The HRCam consists of the detector, mechanical structure, filter wheel and optics. The optics forms an enlarged image on the CCD to enable diffraction-limited resolution. Major parameters of HRCam are listed in table 1.

Table 1: Summary of HRCam parameters

Parameter	Value
Pixel scale, format, FoV	15 mas, 658x496, $9.9'' \times 7.5''$
Signal resolution, gain	14 bits (16384 ADU), 1.7 el/ADU
Readout noise	14.3el or 8.4 ADU
QE, EM gain	Max. 0.5, gain 1–440
Readout speed	30 FPS full-frame
Filters	U, B, V, R, I, Hα

This document contains an essential information on the HRCam hardware. The software for data ascquisition and instrument control is described in a separate manual. Table 2 lists commercial HRcam components.

Table 2: Commercial components of HRCam

Component	Vendor	Cost, USD
Luca DL658 CCD camera	andor.com	9000
Filter wheel CFW10-SA	sbig.com	995
UBVRI $1.25''$ filters	sbig.com	875
Hα $1.25''$ 4.5nm	sbig.com	275
Two 25-mm lenses	edmundoptics.com	133

2 Detector

The detector model is DL-658M-TIL, serial No. DL-098. It is manufactured by Andor Technology (http://www.andor.com). Major parameters according to the manufacturer's data and our own study are listed in Table 1.

The **mechanical interface** of the detector is a standard C-mount (thread of 1" diameter, 32 TPI). The C-mount has a standard detector depth of 0.7" (17.6 mm), counting from the front flange. This corresponds to using the Luca with its interface ring. The ring must be removed for use with HRCam, in this case the detector depth is reduced by 5.0 mm and corresponds to the CS-mount standard (0.5" depth).

The CCD is of line-transfer type, which means that very short (0.5 ms?) exposures are possible without mechanical shutter. It is front-illuminated and has moderate quantum efficiency. The physical pixel size is 10x10 μm, the detector sensitive area is thus 6.6x4.9 mm.

The readout speed is 12.5 MHz per pixel, permitting full-frame acquisition rate of 30 fps (126 fps for 128x128 ROI readout). The camera has a USB 2.0 interface. The vendor supplies an image acquisition software for Windows, *SOLIS*, and a software development kit (SDK) for Windows and Linux.

The **EM gain** can be adjusted from 0 (normal CCD operation without gain) to 255. These *gain settings* g are related to the actual EM gain g_e in a non-linear way. Our study has established the following empirical relation:

$$\log_{10} g_e = 0.310 + 1.92E-3g + 2.37E-5g^2. \quad (1)$$

For example, $g = 1, 100, 200, 255$ corresponds, respectively, to $g_e = 2, 5.5, 44, 440$ (the formula is no longer valid for $g = 255$).

The **dark current** is very non-uniform. The detector is normally cooled to $-20°$C thermoelectrically. At this temperature, some 540 "hot pixels" can be identified with high dark currents. About 80% of hot pixels have the dark current less than 62 el/s. The dark current averaged over all pixels is about 0.1 el/s, while the manufacturer specifies it as < 1 el/s.

The signal normally contains a constant offset (**bias**) of +500 ADU. This offset is fairly "flat" and constant. However, when reading in the *kinetic mode* (fast series of frames), only the first frame has this well-defined bias, while the remaining frames show a characteristic bias structure in the vertical direction (Fig. 1).

The **cosmetic quality** of the detector is quite good. Figure 2 shows the flat field image acquired in the laboratory on October 19, 2007. We see a structure in the vertical direction with a period of exactly 41 pixels. The overall rms fluctuation is only 0.61%, the total range is from -3.0% (black spot) to +1.6%.

The **quantum efficiency** curve provided by the manufacturer is reproduced in Fig. 3. The QE below 400 nm is not specified. However, we did not detect bright stars in the U filter, so the detector is essentialy blind in the UV.

3 Optical design

The image at the SOR focal plane is magnified by 2 times to reach the pixel scale of 15 mas (effective focal length 136 m). Such magnification can be easily achieved with one negative lens. However, a

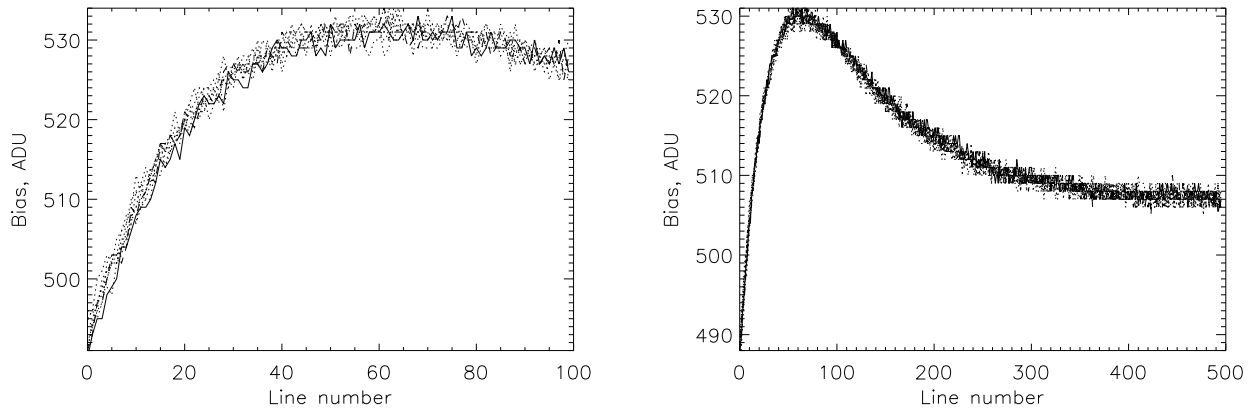

Figure 1: Median bias profile in a 100x100 ROI (left) and full frame (right). In both cases gain setting $g = 100$.

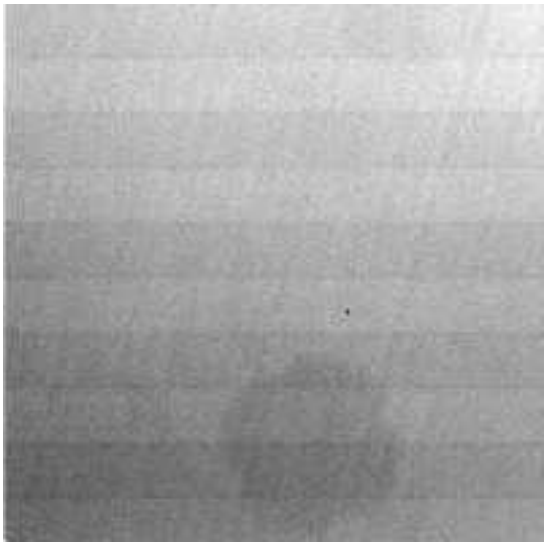

Figure 2: Flat field of Luca. The central 200x200 pixel region with gain setting $g = 100$.

2-lens magnifier with a collimated beam between the lenses is also possible. The advantage of this solution, `HRcam8.zmx`, is that the insertion or removal of the user filters does not change the focus. The layout is shown in Fig. 4 and the prescription in Table 3. The optical quality is very good, 21 nm rms in the spectral bandwidth from 500 nm to 800 nm. The distance between the lenses can be changed freely. By replacing the last lens, we can get different magnification factors if necessary.

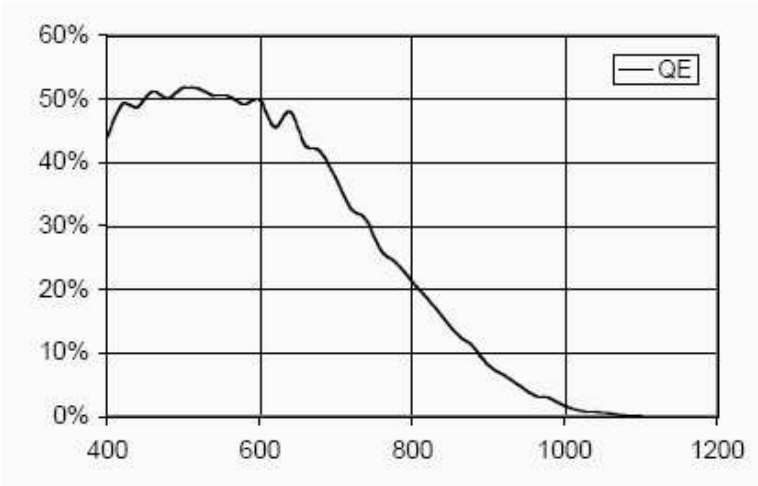

Figure 3: Quantum efficiency of Luca as provided by the manufacturer.

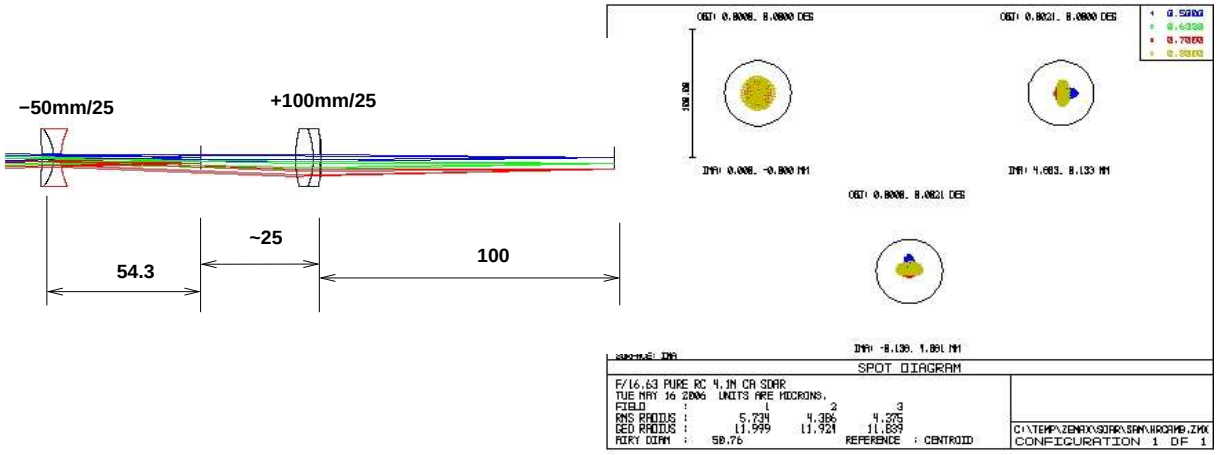

Figure 4: Optical layout of the design `HRcam8.zmx` (left) and the spot diagrams for center and 7.5″ offsets (right).

4 Mechanical design and installation

A fragment of the assembly drawing is shown in Fig. 5. HRCam is normally attached to the SOAR with a big round flange. There are 12 holes on 600 mm diameter for M12 screws. The smaller cylindric base is bolted to the flange with 8 M6 screws on 140 mm diameter. The base contains a negative lens in its holder. The collimated beam after the lens goes through the slide for a user filter and the filter wheel. The slide has a square space of 78.2x78.2 mm width and 10 mm depth. A smaller user filter can be mounted there with a mechanical insert. The slide is fixed with 4 captive screws.

The 10-position filter wheel is manufactured by SBIG and contains 1.25″ filters in standard SBIG threaded mounts (glass diameter 28 mm). In order to access the filters for changing or cleaning, the HRCam must be disassembled. We had a problem with the wheel rotation when its axis was not

Table 3: Optical prescription for `HRcam8.zmx`

Element	Distance to the next, mm
SAM focus	−54.3
EO 45221, −50/25	80 (variable)
EO 32327, +100/25	95.92
CCD focal plane	–

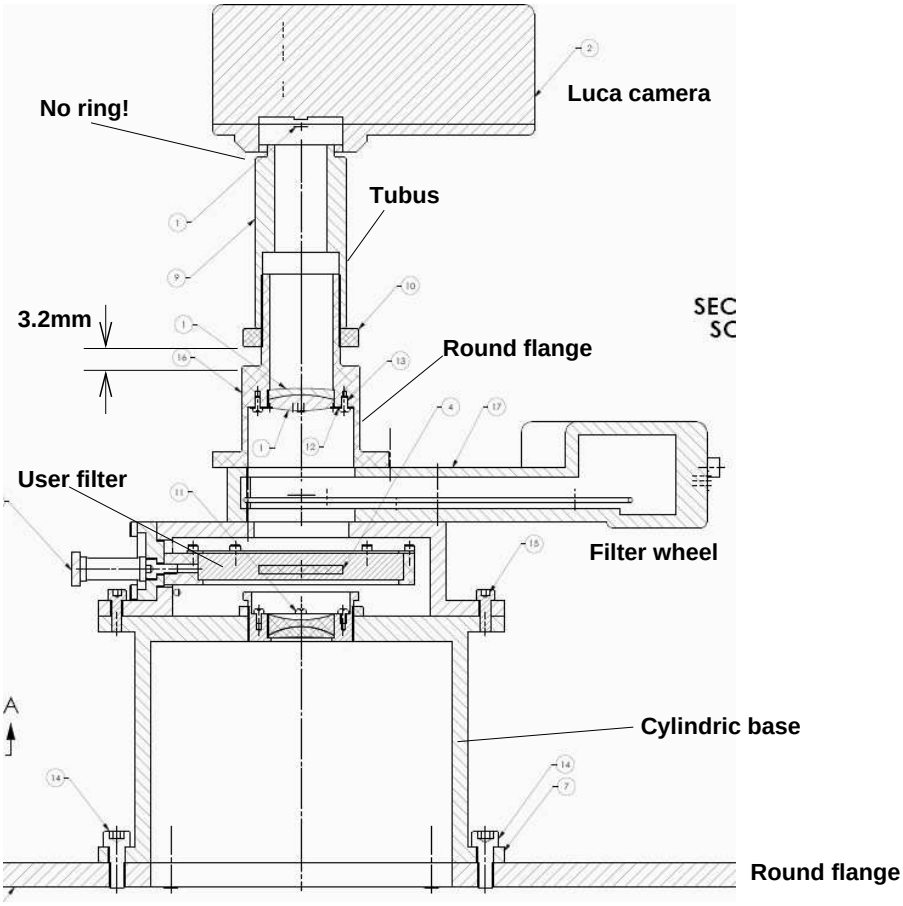

Figure 5: Fragment of the HRCam assembly drawing CH2041-1000-00040.pdf.

tightened.

The round flange with positive lens is bolted to the filter wheel with 4 M4 screws. There are two sets of M4 threaded holes, use those with deeper thread. Be careful to use the screws of adequate length (8 mm), otherwise they will protrude inside the wheel and will stuck or damage the filters. The distance between the detector and the positive lens can be adjusted by rotating the threaded tubus and fixing it with a locking nut. By focusing the collimated beam in the laboratory, we determined that the gap between the nut and the flange must be 3.2 mm. To adjust the detector position angle,

we unlock the nut, rotate slightly the tubus with respect to the flange, and lock the nut again. Be sure that the detector is threaded on the tubus without excessive force, but firmly enough to prevent its rotation at the telescope.

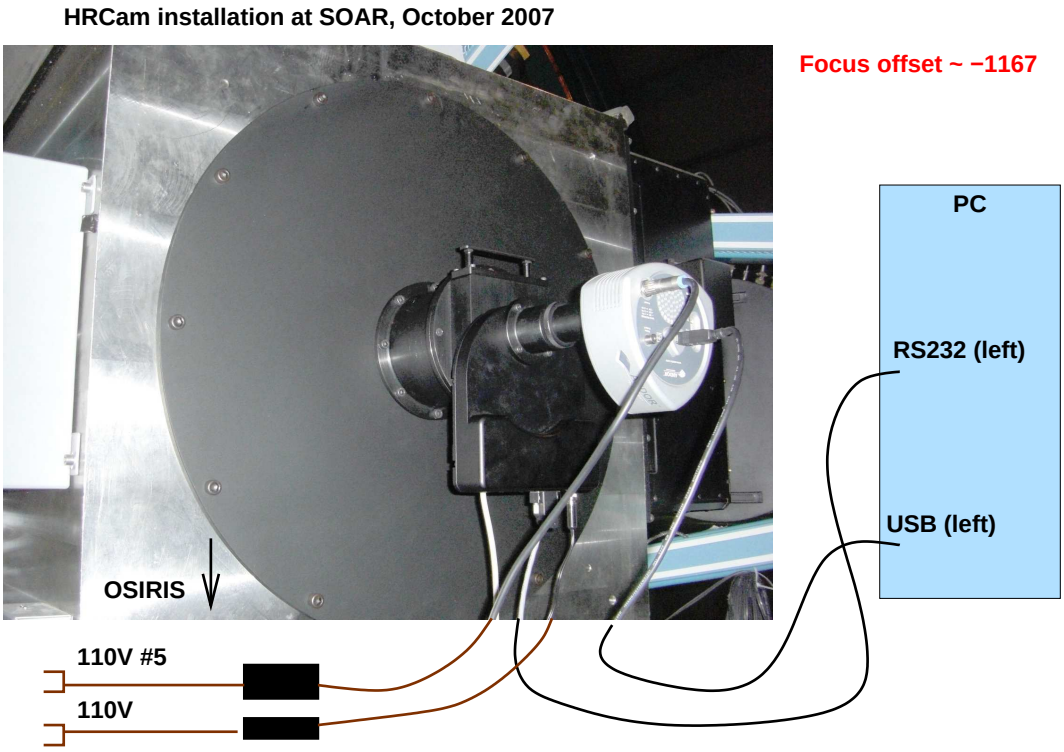

Figure 6: HRCam installed at the IR straight port of the SOAR, and its connections.

A picture of HRcam at SOAR is shown in Fig. 6. Both camera and the filter wheel "look" in the direction of OSIRIS. This orientation can be changed in the future. Direct attachment to the straight IR port requires refocusing the SOAR M2 by ∼1 mm, so that the SOAR guider cannot be used.

5 Filter characteristics and photometry

The filters installed in HRCam were measured by R. Tighe on Nov. 13, 2007 using the CTIO filter-measuring setup. The transmission curves are plotted in Fig. 7, their main characteristics are listed in Table 4, with all wavelengths in nm. The bandwidth $\Delta\lambda_{FWHM}$ is determined at the level of half-transmission, the equivalent bandwidth $\Delta\lambda_{EW}$ is calculated as the integral of the transmision curve divided by the maximum transmission. The positions of the filters in the filter wheel are given as well. Originally, the U-filter was installed in the slot 2, but it is useless because the detector cutoff is outside the filter bandpass. The U-filter was replaced in May 2008 with the Strömgren Y-filter (Fig. 8) which was cut form an old 2-inch square filter available at CTIO. The response of the Hα filter is shifted slightly to the red with respect to the Hα line at 656.3 nm.

The photometric response of HRCam was determined by observing standard stars in the Graham

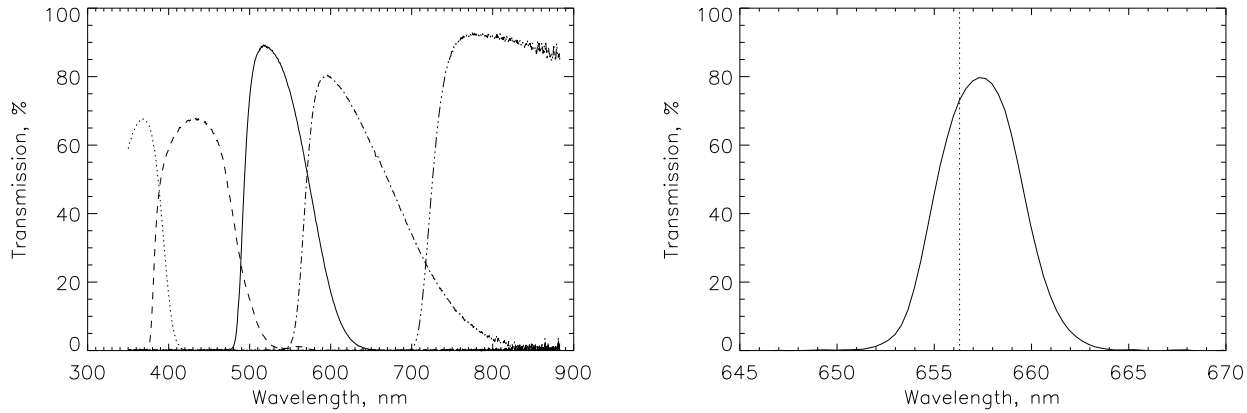

Figure 7: Transmission curves of HRCam filters UBVRI (left) and Hα (right). The vertical line marks the Hα wavelength.

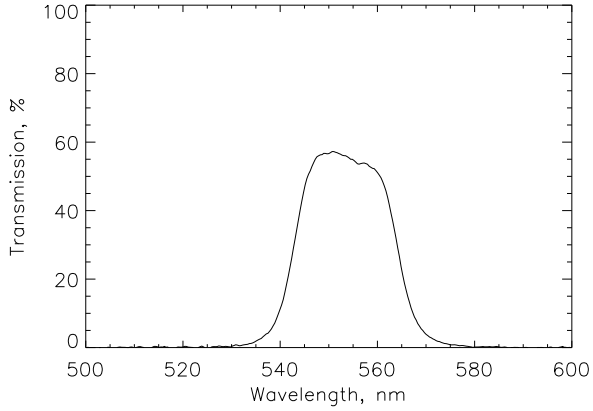

Figure 8: Transmission curve of the Y-filter.

E9 region on October 31, 2007. The relation between the recorded flux F (in ADU per second) and the stellar magnitudes m can be expressed as

$$\log F = -0.4(m - m_0), \tag{2}$$

where m_0 is the instrument zero point for a given filter. This is a magnitude of a star that gives flux one ADU/s. The zero points were determined by averaging the two brightest stars. Once the zero points are known, the fluxes can be converted to the instrumental magnitudes by inverting the relation (2). For each filter, we have useful data on 3 stars and calculate one zero point, hence can evaluate the rms difference between the instrumental and catalog magnitude σ which was from 0.01^m to 0.06^m. The zero point for the Hα filter was inferred indirectly by comparing the counts with the R-filter on a bright star. The zero points are given in the last column of Table 4. Considering the small number of stars observed, we did not attempt to study the photometric system of HRCam.

Table 4: Filter characteristics and zero points

Pos.	Band	T_{max},%	λ_{max}	$\lambda\lambda_{0.5}$	$\Delta\lambda_{FWHM}$	$\Delta\lambda_{EW}$	m_0
2	Y	57.2	550.7	542.7–564.2	21.6	21.8	
3	B	67.8	433.6	383.9–483.0	99.1	97.7	-
4	V	89.2	517.2	492.5–576.7	84.2	84.2	25.27
7	R	80.4	596.1	567.6–688.8	121.2	126.2	25.28
8	I	93.0	774.4	-	-	-	24.44
9	Hα	79.7	657.3	654.8–659.8	5.04	5.05	21.9:

We compare the measured fluxes in the V band with the expected ones to evaluate the detector quantum efficiency (QE). In calculating the expected fluxes, we adopted telescope diameter 4.1 m, central obstruction 0.24, mirror reflectivity 0.89 (3 mirrors), filter bandwidth 84 nm and transmission 0.892. With these data, we expect 6.6E10 photons/s from a star of $V = 0$. The star with $V = 25.28$ (zero point) will give flux 5.1 el/s, while the detector measures the flux 1 ADU/s or 1.7 el/s. The ratio corresponds to the quantum efficiency of 0.33. This estimate is affected by the adopted mirror reflectivity, atmospheric transmission, and the energy distribution in stellar spectra.